1521-0103/362/2/296–305$25.00
THE JOURNAL OF PHARMACOLOGY AND EXPERIMENTAL THERAPEUTICS

https://doi.org/10.1124/jpet.117.241901
J Pharmacol Exp Ther 362:296–305, August 2017

Cannabinoid CB_2 Agonist GW405833 Suppresses Inflammatory and Neuropathic Pain through a CB_1 Mechanism that is Independent of CB_2 Receptors in Mice

Ai-Ling Li, Lawrence M. Carey, Ken Mackie, and Andrea G. Hohmann

Department of Psychological and Brain Sciences (A-L L, L.M.C., K.M., A.G.H.), Program in Neuroscience (L.M.C., K.M., A.G.H.), Gill Center for Biomolecular Science (K.M., A.G.H.), Indiana University, Bloomington, Indiana

Received April 4, 2017; accepted June 2, 2017

ABSTRACT

GW405833, widely accepted as a cannabinoid receptor 2 (CB_2) agonist, suppresses pathologic pain in preclinical models without the unwanted central side effects of cannabinoid receptor 1 (CB_1) agonists; however, recent in vitro studies have suggested that GW405833 may also behave as a noncompetitive CB_1 antagonist, suggesting that its pharmacology is more complex than initially appreciated. Here, we further investigated the pharmacologic specificity of in vivo antinociceptive actions of GW405833 in models of neuropathic (i.e., partial sciatic nerve ligation model) and inflammatory (i.e., complete Freund's adjuvant model) pain using CB_2 and CB_1 knockout (KO) mice, their respective wild-type (WT) mice, and both CB_2 and CB_1 antagonists. GW405833 (3, 10, and 30 mg/kg i.p.) dose dependently reversed established mechanical allodynia in both pain models in WT mice; however, the antiallodynic effects of GW405833 were fully preserved in CB_2KO mice and absent in CB_1KO mice. Furthermore, the antiallodynic efficacy of GW405833 (30 mg/kg i.p.) was completely blocked by the CB_1 antagonist rimonabant (10 mg/kg i.p.) but not by the CB_2 antagonist SR144528 (10 mg/kg i.p.). Thus, the antinociceptive properties of GW405833 are dependent on CB_1 receptors. GW405833 (30 mg/kg i.p.) was also inactive in a tetrad of tests measuring cardinal signs of CB_1 activation. Additionally, unlike rimonabant (10 mg/kg i.p.), GW405833 (10 mg/kg, i.p.) did not act as a CB_1 antagonist in vivo to precipitate withdrawal in mice treated chronically with Δ^9-tetrahydrocannabinol. The present results suggest that the antiallodynic efficacy of GW405833 is CB_1-dependent but does not seem to involve engagement of the CB_1 receptor's orthosteric site.

Introduction

Cannabinoids exhibit antinociceptive effects in behavioral and electrophysiologic studies in rodents (Iversen and Chapman, 2002; Guindon and Hohmann, 2009). Two well characterized cannabinoid receptors are cannabinoid receptor 1 (CB_1) (Matsuda et al., 1990) and cannabinoid receptor 2 (CB_2) (Munro et al., 1993). Agonists that bind to CB_1 receptors have many desirable therapeutic properties, but they also induce undesirable psychoactive side effects that result from the abundant expression of CB_1 receptors in the central nervous system (CNS) (Herkenham et al., 1991; Galiègue et al., 1995). By contrast, CB_2 receptors are restricted mainly to the periphery and immune tissues (Galiègue et al., 1995) but may nonetheless be induced in the CNS by inflammation or injury (Zhang et al., 2003; Guindon and Hohmann, 2008; Viscomi et al., 2009; Atwood and Mackie, 2010). Therefore, much research interest has emerged in developing CB_2 agonists as suitable analgesics.

GW405833 (also known as L768242; see Fig. 1) binds with preferential affinity to CB_2 over CB_1 receptors (Gallant et al., 1996; Valenzano et al., 2005; Yao et al., 2008) (Table 1). Antihyperalgesic effects of GW405833 were first described in a carrageenan model of inflammatory nociception (Clayton et al., 2002). GW405833 was subsequently shown to reduce allodynia in other inflammatory pain (Valenzano et al., 2005; Whiteside et al., 2005; Beltramo et al., 2006), traumatic nerve injury (Valenzano et al., 2005; Whiteside et al., 2005; Beltramo et al., 2006; Brownjohn and Ashton, 2012; Hu et al., 2009; Leichsenring et al., 2009), and incisional injury (LaBuda et al., 2005; Valenzano et al., 2005) models. Despite substantial penetration to the CNS (Bouchard et al., 2012), GW405833 did not produce cannabimimetic deficits at doses lower than 100 mg/kg i.p. (Valenzano et al., 2005; Whiteside et al., 2005). Antiallodynic efficacy of GW405833 was opioid independent as systemic administration of naltrexone did not block the antihyperalgesic or antinociceptive effects of GW405833 (Whiteside et al., 2005). Thus, GW405833 was advanced as a more specific CB_2 agonist compared with AM1241, which exhibited naloxone sensitivity under some (Ibrahim et al., 2005), but not all, conditions (Rahn et al., 2010) and showed substantial protean agonism (Yao et al., 2006).

In in vitro studies, GW405833 was reported to behave as a partial agonist at human CB_2 receptors (Valenzano et al., 2005) and, alternately, a potent inverse agonist at both human

This work was supported by National Institutes of Health National Institute on Drug Abuse Grants DA041229 (to A.G.H. and K.M.), DA009158 (to K.M. and A.G.H.), and DA021696 (to K.M.). L.M.C. is supported by T32 National Institutes of Health National Institute on Drug Abuse training grant DA024628 and the Harlan Scholars Research Program.
https://doi.org/10.1124/jpet.117.241901.

ABBREVIATIONS: ANOVA, analysis of variance; CB_1 or CB_2, cannabinoid receptor 1 or 2; CFA, complete Freund's adjuvant; CNS, central nervous system; KO, knockout; PSNL, partial sciatic nerve ligation; Δ^9-THC, Δ^9-tetrahydrocannabinol; WT, wild type.

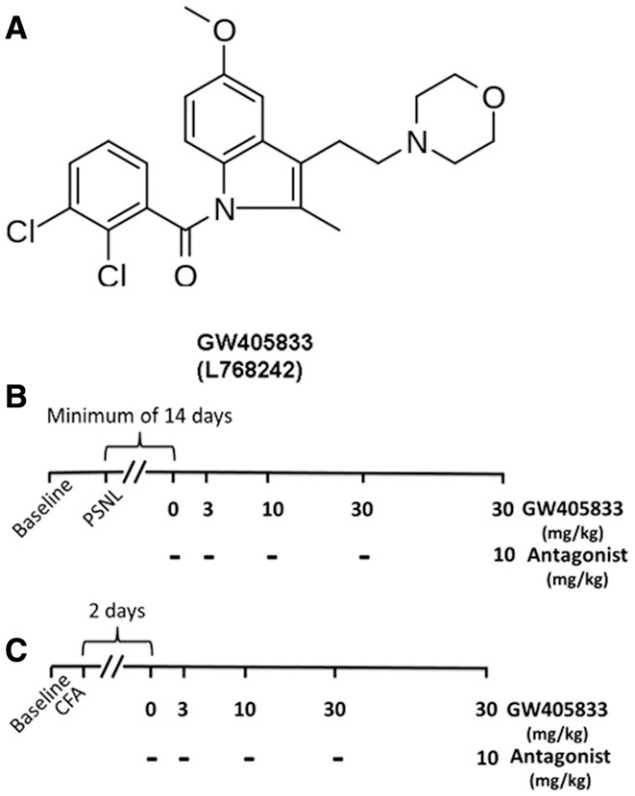

Fig. 1. (A) Chemical structure of GW405833, also referred to as L768242 (Gallant et al., 1996; Valenzano et al., 2005). Cayman Chemical (cat. no. 20219) and Tocris Bioscience (cat. no. 2374) identify this ligand as a selective, high-affinity CB_2 receptor partial agonist. (B and C) Timeline for the dose response of GW405833 and blockade with antagonist in PSNL and CFA model. (B) In the PSNL model, the baseline was tested a day before the surgery. Animals were allowed (≥14 days) to fully develop neuropathic pain before pharmacologic manipulations. After the full establishment of neuropathic pain, different doses of GW405833 were tested in ascending order with variable intervals to ensure no carryover effect. Specifically, 0 mg/kg was tested, followed by 3 mg/kg on the same day with 3- to 4-hour intervals; 10 mg/kg was then tested the next day, followed by 30 mg/kg tested 2 days later. The CB_1 or CB_2 antagonist was tested 3 or 4 days after the last dose of 30 mg/kg. Groups: C57BL/6J, n = 6 (males); CB_2KO, n = 6 (males); CD1, n = 8 (mixed sex); CB_1KO, n = 8 (mixed sex). (C) In the CFA model, the baseline was tested on the same day before the CFA injection; the test of dose response started 48 hours after the injection. The timeline for the dose response of GW405833 was the same as the timeline in PSNL model. Groups: C57BL/6J, n = 8 (mixed sex); CB_2KO, n = 8 (mixed sex); CD1, n = 8 (males); CB_1KO: n = 6 (males).

and rat CB_2 receptors and weak agonist at rat CB_1 receptors (Yao et al., 2008). GW405833 was further proposed to be a protean agonist whose pharmacologic properties were dependent on the constitutive activity of the CB_2 receptor (Mancini et al., 2009). More recently, GW405833 was suggested to act as a noncompetitive CB_1 antagonist as GW405833 noncompetitively antagonized CP55,940-induced adenylyl cyclase activity, extracellular signal-regulated kinase 1/2 phosphorylation, phosphatidylinositol 2 signaling, and CB_1 internalization in vitro in human embryonic kidney cells transfected with CB_1 and showed a complex, time-dependent effect on arrestin recruitment in Chinese hamster ovary cells (Dhopeshwarkar et al., 2017).

Antiallodynic effects of GW405833 have been reported in several preclinical pain models, but pharmacologic specificity has been poorly characterized, and discrepancies among studies do exist. In a few studies, the antihyperalgesic effect of GW405833 was blocked by the CB_2 antagonist SR144528 (Clayton et al., 2002; Beltramo et al., 2006), whereas the effects of GW405833 did not differ from vehicle in CB_2 KO mice (Valenzano et al., 2005). The possible involvement of CB_1 was never investigated in these studies. By contrast, the antinociceptive effect of GW405833 in reducing lactic acid–stimulated stretching was partially blocked by the CB_1 antagonist rimonabant but not by the CB_2 antagonist SR144528, whereas GW405833-induced attenuation of acid-induced depression of intracranial self-stimulation was not blocked by either SR144528 or rimonabant (Kwilasz and Negus, 2013). Because of these discrepancies, we elected to further characterize the pharmacologic specificity of GW405833 in two mechanistically distinct animal pain models, neuropathic pain induced by partial sciatic nerve ligation (PSNL) and inflammatory pain induced by intraplantar injection of complete Freund's adjuvant (CFA). To characterize pharmacologic specificity of the in vivo profile of GW405833, we used CB_2 KO, CB_1KO, and respective wild-type (WT) mice, as well as CB_1 and CB_2 antagonists. The highest effective dose of GW405833 (30 mg/kg i.p.) was also evaluated for cardinal signs of CNS CB_1 activation in the cannabinoid tetrad of tests. GW405833 also behaved as noncompetitive CB_1 antagonist in vitro (Dhopeshwarkar et al., 2017), but it remains unclear whether the reported in vitro effects could account for the pharmacologic effects of this compound observed in vivo. We therefore also evaluated whether GW405833 would behave similarly to the CB_1 antagonist rimonabant and precipitate a withdrawal syndrome in mice treated chronically with Δ^9-tetrahydrocannabinol (Δ^9-THC).

Materials and Methods

Subjects

Mice (5 ± 2 months old) of both sexes from different strains were used as specified in each study. CB_2KO mice and WT littermates on a C57BL/6J background (The Jackson Laboratory, Bar Harbor, ME) and CB_1KO mice and WT mice on a CD1 background (Charles River Laboratories, Wilmington, MA) were included. Animals were single-housed at relatively constant temperature (73 ± 2°F) and humidity (45%) under light-dark cycles of 12/12 hours. All the experimental procedures were approved by Bloomington Institutional Animal Care and Use Committee of Indiana University and followed the guidelines for the treatment of animals of the International Association for the Study of Pain (Zimmermann, 1983).

Drugs and Chemicals

GW405833 was purchased from two different commercial sources (Tocris Bioscience, Bristol, UK, and Cayman Chemical Company, Ann Arbor, MI). CFA and WIN55,212-2 were purchased from Sigma-Aldrich (St. Louis, MO). Rimonabant (SR141716A), SR144528, and Δ^9-THC were obtained from the National Institutes of Health Drug Supply Program (Research Triangle Institute, Research Triangle Park, NC). All drugs except Δ^9-THC were dissolved in a vehicle of dimethylsulfoxide (Sigma-Aldrich, St. Louis, MO), emulphor (Alkamuls EL 620L, Solvay, Princeton, NJ), ethanol (Sigma-Aldrich), and sterile saline (Aquilite System, Hospira Inc, Lake Forest, IL) at a ratio of 5:2:2:16, respectively. Δ^9-THC was dissolved in a vehicle of 95% ethanol, Cremophor EL (Sigma-Aldrich), and sterile saline (Aquilite System) in a ratio of 1:1:18, respectively. All compounds were delivered via i.p. injection in a volume of 5 ml/kg.

TABLE 1
In vitro binding profile of GW405833

Ki (nM)					rCB_2/rCB_1 Selectivity	Assay	Reference
hCB_1	hCB_2	hCB_2/hCB_1 Selectivity	rCB_1	rCB_2			
4772	3.92	1217	273	3.6	76	[^{3}H] CP55,940 binding	Valenzano et al., 2005
282	7.62	37	NA	11.1	NA	[^{3}H] CP55,940 binding	Yao et al., 2008
1917	12	160	NA	NA	NA	[^{3}H] WIN55,212-2 binding	Gallant et al., 1996

NA, not available; hCB, human cannabinoid receptor; rCB, rat cannabinoid receptor.

PSNL

PSNL was performed to induce neuropathic pain. Mice were anesthetized with isoflurane (5% for induction followed by 2%–2.5% for maintenance) in 1.5 liter/min of oxygen. The right high thigh area was then shaved and disinfected, followed by a 1- to 1.5-cm longitudinal incision. The muscle layers were bluntly dissected to expose the underlying sciatic nerve. One third to half of the sciatic nerve at the location just above its trifurcation was tightly ligated using 8-0 silk suture (Sharpoint DA-2526N). The muscle layers were then closed with 5-0 silk thread (Ethicon 682 G; Ethicon Inc., Somerville, NJ), and the skin was closed by staples (Autoclips 9 mm no. 7631). Animals were allowed at least 2 weeks to recover and fully develop neuropathic pain.

CFA-Induced Inflammatory Pain

A single intraplantar injection was used to deliver CFA (20 μl; diluted 1:1 in sterile saline) unilaterally into the right hind paw. Animals were given 48 hours to fully develop inflammatory pain before pharmacologic manipulations.

Assessment of Mechanical Allodynia

Animals were habituated in individual transparent Plexiglass test chambers (10.5 × 9 × 7 cm) atop a metal mesh platform for at least 30 minutes before the testing. An electronic von Frey anesthesiometer with a 90-g probe (IITC Life Science, Woodland Hills, CA) was used to determine the paw withdrawal threshold to mechanical stimulation of the hind paw. A rigid tip with a diameter of 0.8 mm attached to the probe was applied vertically against the plantar surface of the paw with gradually increasing force. The force in grams necessary to produce paw withdrawal was recorded in duplicate for each paw.

Baseline mechanical paw withdrawal thresholds were measured in each paw for each animal before performing either PSNL or injecting CFA. Another predrug baseline was then taken after painful peripheral neuropathy or inflammatory pain was fully established. GW405833 was administered (i.p.) 30 minutes before evaluation of the impact of drug manipulations on mechanical paw withdrawal thresholds. Different doses of GW405833 were injected (i.p.) within subjects in the order of vehicle (0), 3, 10, and 30 mg/kg. Sufficient time was allowed to lapse between each dose to verify that mechanical paw withdrawal thresholds returned to the predrug levels before dose escalation. (For detailed timeline information, please see Fig. 1, B and C). In the groups where CB_1 or CB_2 antagonists were tested, rimonabant or SR144528 (10 mg/kg i.p.) was administered 20 minutes before GW405833 injection.

Tetrad Test

Rotarod. Motor performance was measured using an accelerating Rotarod (IITC Life Science) (4–40 rpm, 300-second cutoff time). Male CD1 mice were trained over 2 consecutive days, and on day 3, the baseline latencies to descend from the rotating drum were measured. Mice that did not meet exclusion criteria before baseline measurements (i.e., ability to stay on rotating drum for at least 30 seconds on baseline day) were removed from the study and did not receive pharmacologic treatments.

Rectal Temperature. Rectal temperature was measured to assess hypothermia by insertion of a mouse rectal probe (Braintree Laboratories Inc., Braintree, MA) 1.2 cm into the rectum using a thermometer (Physitemp Instruments Inc., Clifton, NJ).

Tail-Flick Test. To assess the effects of drug treatments on acute antinociception, mice were gently restrained in a towel, and the tip of the tail (~1 cm) was submerged in a hot water bath maintained at 54 to 55°C. The latency to withdraw the tail was measured.

Ring Test. The ring test (Pertwee, 1972) was performed to assess possible cataleptic effects produced by drug administration. Briefly, each mouse was positioned on top of an elevated ring attached to a vertical stainless steel rod suspended at a height of 16 or 17 cm above a flat platform for a total duration of 5 minutes. The amount of time spent immobile was recorded as an index for catalepsy.

Behavioral Assessment of the Development of Tolerance to Δ^9-THC

Male mice of the C57 background strain received once-daily injections of Δ^9-THC (50 mg/kg i.p.) for 9 consecutive days. Mice were assessed in three of the behavioral assays from the tetrad test to quantify the development of tolerance to the behavioral effects of Δ^9-THC. Motor coordination was measured using the rotarod test, body temperature was measured using a rectal temperature probe, and antinociception was measured using the tail-flick test. Responses were measured at baseline and 30 minutes after administration of Δ^9-THC on days 1 and 8 of Δ^9-THC administration. Mice received Δ^9-THC in the same environment each day and remained for 4 hours post-Δ^9-THC injection before being returned to the colony room.

Assessment of Antagonist-Precipitated Withdrawal Symptoms in Δ^9-THC–Treated Mice

On day 9 of Δ^9-THC administration, all mice were challenged with vehicle (i.p.), followed 30 minutes later by a second challenge (i.p.) with either rimonabant (10 mg/kg) or GW405833 (10 mg/kg). Mice were placed in clear Plexiglass chambers on an observation platform, and withdrawal behaviors were videotaped and scored by an investigator blinded to treatment conditions. On the day of withdrawal testing, mice were injected with Δ^9-THC (50 mg/kg, i.p.) and allowed to acclimate to the chamber for 30 minutes. Next, all mice received a single injection of vehicle (i.p.), and behavior was videotaped for 30 minutes. Immediately after vehicle challenge, mice received a single i.p. injection of either rimonabant or GW405833, and behavior was videotaped for 30 minutes. The numbers of front paw tremors, headshakes, scratching, grooming, and rearing behaviors were counted. All mice received vehicle, followed by drug challenge so that within-subject comparisons could be made.

Statistical Analysis

Differences in mechanical paw withdrawal thresholds were evaluated using mixed analysis of variance (ANOVA) (with different pharmacologic treatments as the within-subject variable and genotype as between-subject variable), followed by Bonferroni post hoc

tests. For tetrad tests, one-way ANOVA was performed separately on predrug (baseline) and postdrug responses, followed by Bonferroni post hoc tests. Paired or independent t tests were performed with the specific comparisons of interest as indicated. ANOVA for repeated measures was used to determine the time course of tolerance development to the effects of Δ^9-THC, followed by paired-samples t tests to confirm the development of tolerance. Paired samples t tests were used to assess differences in withdrawal symptoms elicited by vehicle versus drug challenge. Statistical analyses were performed using IBM SPSS Statistics version 24 (IBM Corporation, Armonk, NY) or GraphPad Prism version 5.02 statistical software for windows (GraphPad Software, San Diego, CA). Figures were generated using GraphPad Prism version 5.02 statistical software. All data are presented as mean ± S.E.M.; $P < 0.05$ was considered significant.

Results

GW405833-Induced Suppressions of Neuropathic Pain in the PSNL Model Are CB_1 Receptor-Dependent and CB_2 Receptor-Independent

GW405833-Induced Antiallodynic Effects in PSNL Model Are Fully Preserved in CB_2 KO Mice and Are Not Blocked by a CB_2 Antagonist. PSNL lowered mechanical paw withdrawal thresholds in CB_2KO and respective WT mice relative to baseline, consistent with the development of neuropathic pain ($F_{1,10} = 27.434$, $P < 0.001$), but these effects did not differ between WT and CB_2 KO mice ($F_{1,10} = 0.003$, $P = 0.988$) (Fig. 2A). Vehicle (0 mg/kg, i.p.) alone did not alter mechanical paw withdrawal thresholds in either group ($P > 0.05$) (Fig. 2A). ANOVA revealed a main effect of GW405833 treatment on mechanical allodynia ($F_{3,30} = 11.381$, $P < 0.001$), and Bonferroni post hoc tests indicated that GW405833 elevated paw withdrawal thresholds in a dose-dependent manner (Fig. 2A). No main effects of genotype ($F_{1,10} = 3.620$, $P = 0.086$) or significant interactions were observed ($P = 0.598$) (Fig. 2A). These results indicate that the antiallodynic effect of GW405833 was fully preserved in CB_2KO mice. GW405833 (10 and 30 mg/kg i.p.) fully restored mechanical paw withdrawal thresholds relative to baseline at doses as low as 10 mg/kg i.p. in both WT ($t_5 = 0.270$, $P = 0.798$) and CB_2KO ($t_5 = 1.959$, $P = 0.107$) mice (Fig. 2A). Paired t tests indicated that the CB_2 antagonist SR144528 (10 mg/kg i.p.) did not block the antiallodynic efficacy of GW405833 (30 mg/kg i.p.) in CB_2KO mice ($t_5 = 1.790$, $P = 0.133$), but it attenuated the efficacy of GW405833 in WT mice ($t_5 = 2.833$, $P = 0.037$). Although the antiallodynic efficacy of GW405833 (30 mg/kg i.p.) was attenuated in WT mice by SR144528, residual efficacy was nonetheless comparable to that observed in WT mice receiving GW405833 alone at a highly efficacious dose of 10 mg/kg i.p. ($t_5 = 0.800$, $P = 0.460$). Moreover, the antiallodynic efficacy of GW405833 in WT mice did not differ between doses of 10 mg/kg i.p. and 30 mg/kg i.p ($P = 1.0$). These observations suggest that, in WT mice, SR144528-induced blockade of the antiallodynic efficacy of GW405833 was minimal, if present at all.

GW405833-Induced Antiallodynic Effects in PSNL Model Are Absent in CB_1 KO Mice and Are Blocked by a CB_1 Antagonist. PSNL lowered mechanical paw withdrawal thresholds in CB_1KO and respective WT mice relative to baseline, consistent with the development of robust mechanical allodynia ($F_{1,14} = 42.594$, $P < 0.001$), but these effects did not differ between WT and CB_1 KO mice ($F_{1,14} = 1.079$, $P = 0.317$) (Fig. 3A). Vehicle (0 mg/kg, i.p.) did not alter mechanical paw withdrawal thresholds after the neuropathic pain was fully established ($P > 0.05$). There was a main effect of GW405833 on mechanical allodynia ($F_{3,42} = 5.025$, $P = 0.005$), a main effect of genotype ($F_{1,14} = 14.820$, $P = 0.002$), and a trend was observed for the interaction that approached statistical significance ($F_{3,42} = 2.487$, $P = 0.074$) (Fig. 3A). Bonferroni post hoc tests indicated that GW405833 dose dependently elevated mechanical paw withdrawal thresholds in WT mice, but these antiallodynic effects were absent in CB_1KO mice (Fig. 3A). The highest dose of GW405833 (30 mg/kg i.p.) did not fully restore mechanical paw withdrawal thresholds to baseline (preinjury) levels ($t_7 = 3.33$, $P = 0.013$). In WT mice, pretreatment with the CB_1 antagonist rimonabant (10 mg/kg i.p.) before GW405833 (30 mg/kg i.p.) completely blocked the antiallodynic effect of GW405833 ($t_7 = 3.097$, $P = 0.017$), and the resulting mechanical thresholds did not differ from those of CB_1KO mice receiving GW405833 alone (30 mg/kg i.p.) ($t_{14} = -0.582$, $P = 0.597$) (Fig. 3A).

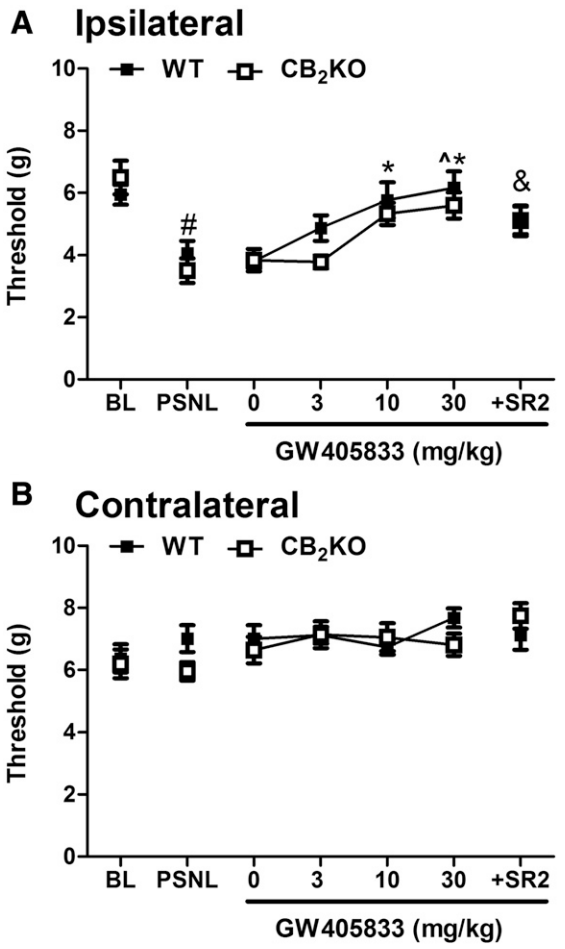

Fig. 2. GW405833 dose dependently reversed PSNL-induced mechanical allodynia in both WT and CB_2KO mice (A). The effect of GW405833 (30 mg/kg i.p.) was only slightly attenuated by pretreatment with the CB_2 antagonist SR144528 (10 mg/kg i.p.). Mechanical thresholds were not changed in the contralateral paw after PSNL or by drug treatments (B). WT (C57BL/6J): $n = 6$ males; CB_2KO: $n = 6$ males. $^{\#}P < 0.05$ vs. baseline; $^{*}P < 0.05$ vs. vehicle (0 mg/kg i.p.); $^{\wedge}P < 0.05$ vs. GW405833 (3 mg/kg i.p.); $^{\&}P < 0.05$ vs. GW405833 (30 mg/kg i.p.) in WT. BL, preinjury baseline. SR2, CB_2 antagonist SR144528; ipsilateral, injured side; contralateral, uninjured side.

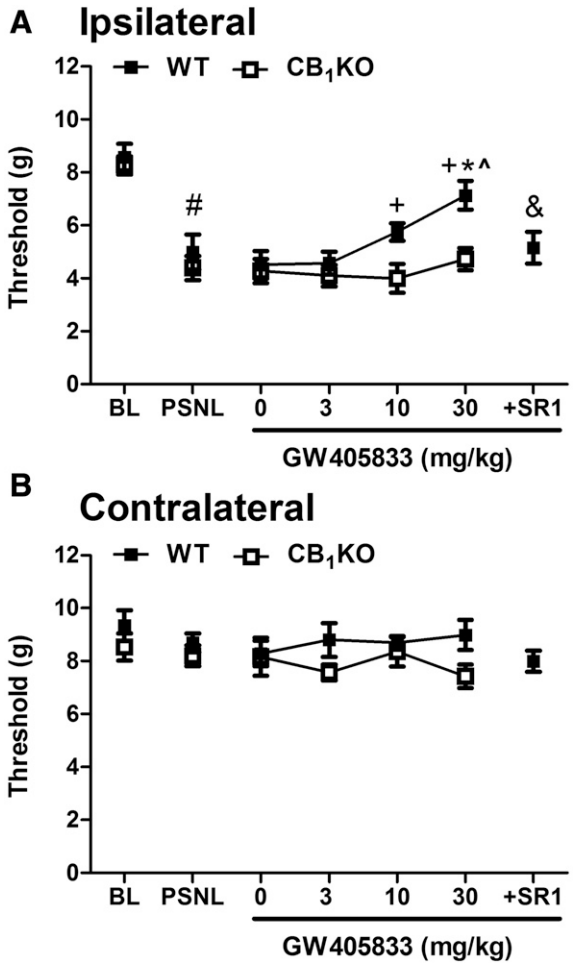

Fig. 3. GW405833 dose dependently reversed PSNL-induced mechanical allodynia in WT but not in CB_1KO mice (A). The antiallodynic effect of GW405833 (30 mg/kg i.p.) was completely blocked by the CB_1 antagonist rimonabant (10 mg/kg i.p.) (A) Mechanical threshold was not changed in the contralateral paw after PSNL or by drug treatments (B). Mixed-sex groups were used; WT (CD1), $n = 8$; CB_1KO, $n = 8$. $P < 0.05$ vs. baseline; $^{*}P < 0.05$ vs. vehicle (0 mg/kg i.p.); $^{\wedge}P < 0.05$ vs. GW405833 (3 mg/kg i.p.); $^{+}P < 0.05$ vs. CB_1KO; $^{\&}P < 0.05$ vs. GW405833 (30 mg/kg i.p.) in WT. BL, preinjury baseline. Ipsilateral, injured side; contralateral, uninjured side.

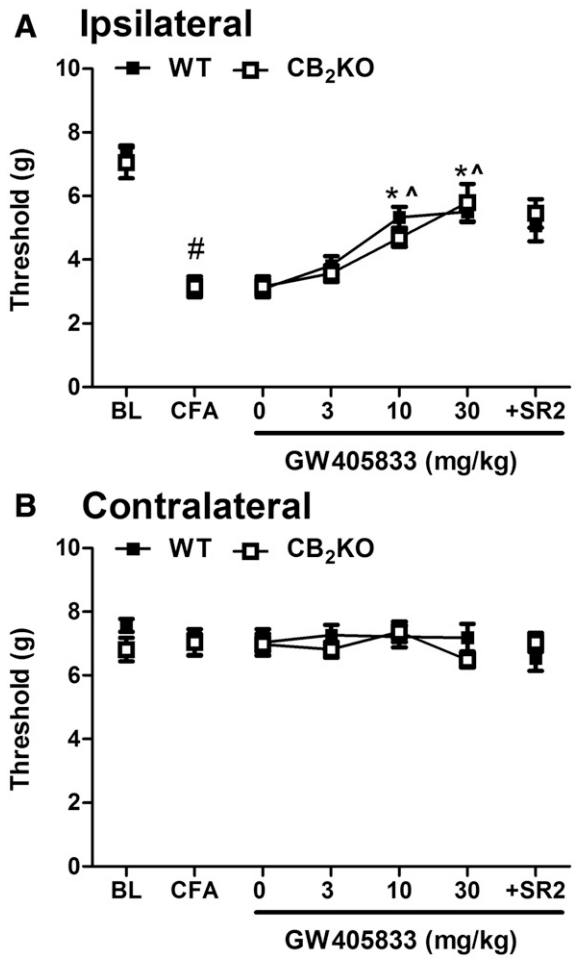

Fig. 4. GW405833 dose dependently reversed CFA-induced mechanical allodynia in both WT and CB_2KO mice (A). The antiallodynic effect of GW405833 (30 mg/kg i.p.) was unaffected by the CB_2 antagonist SR144528 (10 mg/kg i.p.). Mechanical paw withdrawal thresholds in the contralateral paw were not changed by CFA injection or drug treatments (B). Mixed-sex groups were used: WT (C57BL/6J), $n = 8$; CB_2KO, $n = 8$. $^{\#}P < 0.05$ vs. baseline; $^{*}P < 0.05$ vs. vehicle (0 mg/kg i.p.); $^{\wedge}P < 0.05$ vs. GW405833 (3 mg/kg i.p.) BL, preinjection baseline; SR2, CB_2 antagonist SR144528. Ipsilateral, injected paw; contralateral, uninjected paw.

Neither PSNL nor pharmacologic manipulations altered the mechanical thresholds in the contralateral (uninjured) paw in any genotype ($P > 0.27$) (Figs. 2B and 3B).

GW405833-Induced Antiallodynic Effects in the CFA Model of Inflammatory Pain are CB_1 Receptor–Dependent and CB_2 Receptor–Independent

GW405833-Induced Antiallodynic Effects in CFA Model Are Fully Preserved in CB_2 KO Mice and Are Not Blocked by a CB_2 Antagonist. Intraplantar CFA injection reduced mechanical paw withdrawal thresholds in both WT and CB_2KO mice ($F_{1,14} = 222.594$, $P < 0.001$) (Fig. 4A). There was a main effect of GW405833 treatment on mechanical allodynia ($F_{3,42} = 37.257$, $P < 0.001$), and Bonferroni post hoc tests indicated that GW405833 suppressed CFA-induced allodynia in a dose-dependent manner (Fig. 4A). There was no main effect of genotype ($F_{1,14} = 0.146$, $P = 0.708$) or interaction ($F_{3,42} = 1.156$, $P = 0.338$). Efficacy of the 10 mg/kg and 30 mg/kg i.p. doses of GW405833 did not differ from each other ($P = 0.236$). Together, these data indicate that the antiallodynic efficacy of GW405833 was fully preserved in CB_2KO mice relative to WT mice. The highest dose of GW405833 (30 mg/kg i.p.) did not produce a full reversal of mechanical allodynia in WT relative to pre-CFA baseline ($t_7 = 5.024$, $P = 0.002$), but there was no statistically significant difference between pre-CFA baseline and GW405833 (30 mg/kg i.p.)-reversed mechanical withdrawal thresholds in CB_2KO ($t_7 = 2.097$, $P = 0.074$) mice. Moreover, there was no difference in responding between WT and CB_2KO mice ($t_{14} = 0.437$, $P = 0.165$) (Fig. 4A). Paired-samples t tests showed that the CB_2 antagonist SR144528 did not block the antiallodynic efficacy of GW405833 in either WT ($t_7 = 0.858$, $P = 0.419$) or CB_2KO ($t_7 = 0.760$, $P = 0.472$) mice (Fig. 4A).

GW405833-Induced Antiallodynic Effects in CFA Model Are Absent in CB_1 KO Mice and Blocked by a CB_1 Antagonist in WT Mice. Intraplantar CFA injection lowered mechanical paw withdrawal thresholds in both WT and CB_1KO mice, suggesting that both genotypes developed

inflammatory pain ($F_{1,\ 12} = 145.506$, $P < 0.001$) (Fig. 5A). Vehicle (i.p.) did not alter mechanical paw withdrawal thresholds after CFA-induced inflammation was established ($P > 0.05$). There was a main effect of GW405833 treatment on mechanical allodynia ($F_{3,\ 36} = 26.618$, $P < 0.001$), a main effect of genotype ($F_{1,12} = 8.348$, $P < 0.001$), and the interaction was significant ($F_{\ 3,\ 36} = 8.212$, $P = 0.014$) (Fig. 5A). Bonferroni post hoc tests revealed that GW405833 produced a dose-dependent elevation of mechanical thresholds in WT mice, but such antiallodynic effects were absent in CB_1KO mice (Fig. 5A). The highest dose of GW405833 (30 mg/kg i.p.) fully restored mechanical paw withdrawal thresholds relative to baseline (pre-CFA) levels ($t_7 = 1.374$, $P = 0.212$) in WT mice. Moreover, the CB_1 antagonist rimonabant completely blocked the antiallodynic efficacy of GW405833 in WT mice ($t_7 = 5.58$, $P = 0.001$) (Fig. 5A). Mechanical paw withdrawal thresholds observed in CB_1KO mice treated with GW405833 (30 mg/kg i.p.) did not differ from those observed in WT mice pretreated with rimonabant before GW405833 (30 mg/kg i.p.; $t_{12} = 1.150$, $P = 0.189$) (Fig. 5A). Moreover, local administration of GW405833 (30 μg or 300 μg in 10 μl) in the CFA-injected paw of CB_1 KOs did not produce antiallodynic efficacy (data not shown).

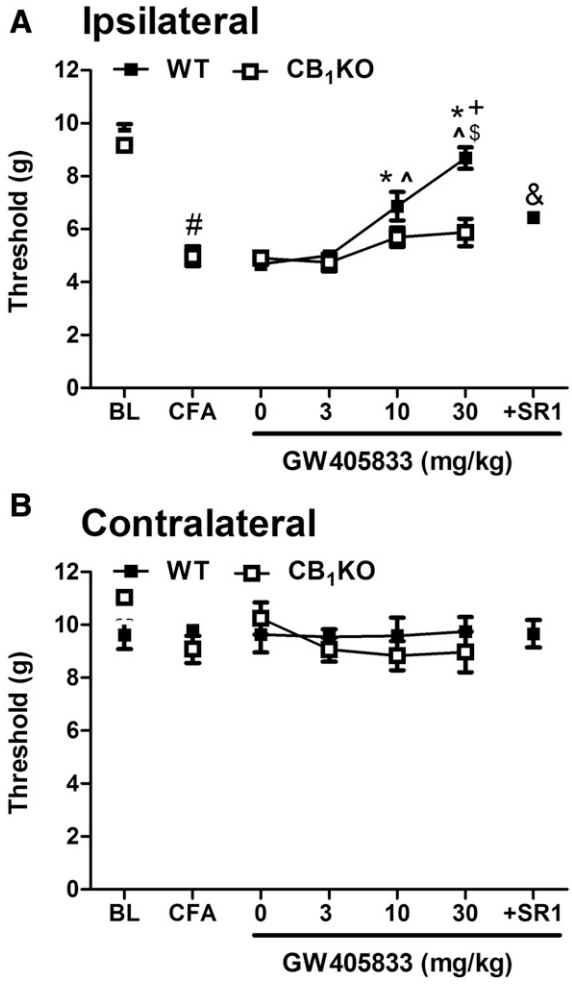

Fig. 5. GW405833 dose dependently reversed CFA-induced mechanical allodynia in WT but not in CB_1KO mice (A). The antiallodynic effect of GW405833 (30 mg/kg i.p.) in WT mice was completely blocked by the CB_1 antagonist rimonabant (10 mg/kg i.p.) (B) Mechanical withdrawal thresholds in the contralateral paw were not changed by CFA injection or treatments (B). WT (CD1), $n = 8$ males; CB_1KO, $n = 6$ males. $^{\#}P < 0.05$ vs. baseline; $^{*}P < 0.05$ vs. vehicle (0 mg/kg i.p.); $^{\wedge}P < 0.05$ vs. GW405833 (3 mg/kg i.p.); $^{\$}P < 0.05$ vs. GW405833 (10 mg/kg i.p.); $^{+}P < 0.05$ vs. CB_1KO; $^{\&}P < 0.05$ versus GW405833 (30 mg/kg i.p.) in WT. BL, preinjection baseline; ipsilateral, injected paw; contralateral, uninjected paw.

Neither CFA injection nor pharmacologic manipulations altered mechanical thresholds in the contralateral (non-inflamed) paw in any genotype ($P > 0.33$) (Figs. 4B and 5B).

GW405833 Does Not Induce Typical Cannabimimetic Effects in the Tetrad Tests

Before pharmacologic manipulations, responding rates did not differ in the three groups in the ring test ($F_{2,\ 15} = 0.344$, $P = 0.715$), rotarod test ($F_{2,15} = 0.027$, $P = 0.973$), rectal temperature assessment ($F_{2,15} = 0.443$, $P = 0.650$), or tail-flick test ($F_{2,15} = 0.411$, $P = 0.670$) (Fig. 6). Pharmacologic manipulations altered postdrug responding in the ring test ($F_{2,15} = 31.010$, $P < 0.001$) (Fig. 6A). Bonferroni post hoc tests revealed that the positive control WIN55, 212-2 (5 mg/kg i.p.) increased immobility in animals compared with the vehicle or GW405833 (30 mg/kg i.p.) injection ($P < 0.001$) (Fig. 6A). Immobility time in the ring test in groups receiving GW405833 did not differ from vehicle ($P = 1.0$) or the preinjection responding ($P = 0.156$) (Fig. 6A). Therefore, GW405833 (30 mg/kg i.p.) failed to induce catalepsy.

Drug manipulations tended to alter rota-rod descend latencies ($F_{2,15} = 3.264$, $P = 0.067$). Nonetheless, planned comparison independent t tests revealed that rotarod latencies were lower in groups receiving WIN55, 212-2 (5 mg/kg i.p.) compared with GW405833 ($P = 0.046$). By contrast, the effects of GW405833 (30 mg/kg i.p.) did not differ from vehicle ($P = 0.302$). Thus, GW405833 at a dose of 30 mg/kg i.p. did not produce motor ataxia in WT mice.

Pharmacologic manipulations altered body temperature ($F_{2,15} = 52.875$, $P < 0.001$). Bonferroni post hoc tests revealed that the positive control WIN55 212-2 (5 mg/kg i.p.) reduced rectal temperature compared with body temperatures measured in mice receiving either vehicle or GW405833 ($P < 0.001$ for each comparison) (Fig. 6C). By contrast, postinjection body temperatures in mice receiving GW405833 did not differ from those observed in mice receiving vehicle ($P = 0.555$) and did not differ from preinjection (baseline) body temperatures ($P = 0.119$) (Fig. 6C). Therefore, GW405833 failed to induce hypothermia.

Pharmacologic manipulations altered postinjection tail-flick latencies ($F_{2,15} = 7.993$, $P = 0.004$). Bonferroni post hoc tests indicated that the positive control WIN55, 212-2 (5 mg/kg i.p.) increased tail-flick latencies compared with either vehicle or GW405833 treatments ($P < 0.05$) (Fig. 6D). By contrast, postinjection tail-flick latencies in groups receiving GW405833 did not differ from vehicle ($P = 0.772$) or the preinjection latency ($P = 0.691$) (Fig. 6D). Therefore, GW405833 failed to induce acute tail-flick antinociception.

Mice Develop Tolerance to Motor Ataxic, Hypothermic, and Antinociceptive Properties of Δ^9-THC

Before withdrawal manipulations, there were no differences between any of the groups in any of the dependent measures used to assess the development of tolerance ($P > 0.1$). Therefore, prewithdrawal responses of all mice were pooled for statistical analysis of tolerance development (Fig. 7).

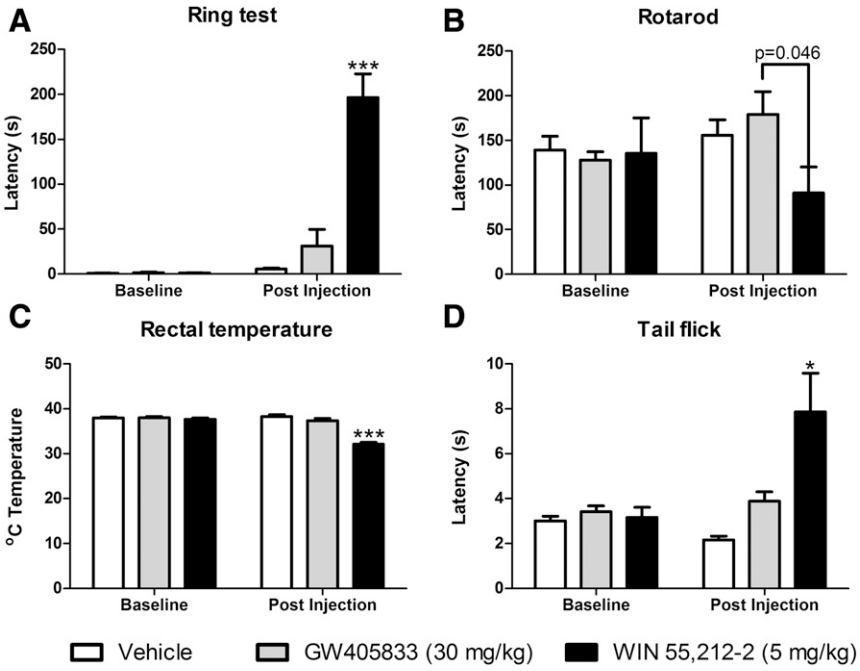

Fig. 6. GW405833 (30 mg/kg i.p.) did not induce catalepsy (A), motor ataxia (B), hypothermia (C), or acute tail-flick antinociception (D) in mice (n = 6 CD1 male mice per group). *$P < 0.05$; ***$P < 0.001$ vs. all the other postinjection groups (vehicle and WIN55, 212-2, 5 mg/kg i.p.).

Mice treated chronically with Δ^9-THC (50 mg/kg/d i.p. × 8 days) exhibited motor impairment ($F_{2,20}$= 108.8, $P < 0.0001$; Fig. 7A), and there was no main effect of group ($P > 0.8$) or interaction ($P > 0.3$). Δ^9-THC produced motor impairment on day 1 of administration relative to baseline (t_{11} = 8.899, $P <$ 0.0001; Fig. 7A), but full tolerance developed by day 8 of drug administration (t_{11} = 12.39, $P < 0.0001$; Fig. 7A), indicating that animals developed tolerance to the motor ataxic effects of Δ^9-THC. Latencies to descend from the rotarod were also higher on day 8 relative to baseline (t_{11} = 6.154, $P < 0.0001$; Fig. 7A), indicating that rotarod performance may have improved with additional training when acute motor impairment from Δ^9-THC was no longer present.

Δ^9-THC decreased rectal temperature ($F_{2,20}$ = 140.2, $P <$ 0.0001; Fig. 7B), and there was no main effect of group ($P >$ 0.3) or interaction ($P > 0.3$). Δ^9-THC decreased rectal temperature on day 1 of administration relative to baseline (t_{11} = 14.66, $P < 0.0001$; Fig. 7B) but reached ~95% tolerance by day 8 of administration (t_{11} = 10.62, $P < 0.0001$; Fig. 7B), indicating that the mice had become tolerant to the hypothermic effects of Δ^9-THC. Δ^9-THC also decreased rectal temperature on day 8 relative to baseline (t_{11} = 2.367, $P < 0.05$; Fig. 7B).

In the hot water tail-flick test, Δ^9-THC treatment (i.p.) produced antinociception in all mice ($F_{2,20}$ = 19.18, $P <$ 0.0001; Fig. 7C), and there was no effect of group ($P > 0.1$) or interaction ($P > 0.4$). Δ^9-THC increased the latency to withdraw the tail on day 1 relative to baseline (t_{11} = 4.644, $P <$ 0.001; Fig. 7C) and responding on day 8 (t_{11} = 4.134, $P < 0.01$; Fig. 7C) of administration. Tail withdrawal latencies did not differ on day 8 of administration relative to baseline ($P > 0.1$), indicative of the development of tolerance to the antinociceptive effects of Δ^9-THC.

Rimonabant Elicits Classic Signs of Cannabinoid Withdrawal, but GW405833 Does Not

In mice chronically treated with Δ^9-THC (50 mg/kg/d × 9 days, i.p.), rimonabant challenge (10 mg, i.p.) increased paw tremors (t_5 = 3.95, $P < 0.05$; Fig. 8A), head shakes (t_5 = 2.716, $P < 0.05$; Fig. 8A), grooming behavior (t_5= 2.963, $P < 0.05$; Fig. 8A) and rearing behaviors (t_5= 3.943, $P < 0.05$, Fig. 8A) relative to vehicle (i.p.) challenge.

In mice chronically treated with Δ^9-THC (50 mg/kg/day × 9 days, i.p.), GW405833 (10 mg/kg, i.p.) decreased paw tremors (t_5 = 3.955, $P < 0.05$; Fig. 8B) but failed to alter head shakes, scratching, grooming, or rearing behaviors ($P > 0.05$) relative to vehicle challenge (i.p.).

Discussion

GW405833 has been widely described in the literature as a cannabinoid CB_2 agonist, although the pharmacological specificity of its in vivo profile of actions has not been thoroughly evaluated. We characterized the pharmacologic specificity of the antiallodynic effects of GW405833 using both neuropathic (i.e., induced by PSNL) and inflammatory (i.e., induced by CFA) pain models in mice. Consistent with other studies (Valenzano et al., 2005; Whiteside et al., 2005), GW405833 dose dependently reversed mechanical hypersensitivity in both neuropathic and inflammatory pain models after systemic administration. GW405833 (3 mg/kg i.p.) did not produce antiallodynic efficacy, but doses of 10 and 30 mg/kg i.p. robustly reversed established allodynia. PSNL, CFA, and GW405833 treatment did not alter mechanical thresholds in the contralateral paw, suggesting that GW405833 suppressed established allodynia induced by neuropathic or inflammatory insults without altering basal nociceptive thresholds observed in the absence of injury.

The most striking observation of our study was that the antiallodynic efficacy of GW405833 was not meditated by CB_2 receptors. GW405833-induced antinociception was, in fact, fully preserved in CB_2 KO mice in models of established neuropathic and inflammatory pain. GW405833 reversed established allodynia with similar efficacy in WT and CB_2KO mice in both pain models. By contrast, antiallodynic efficacy of

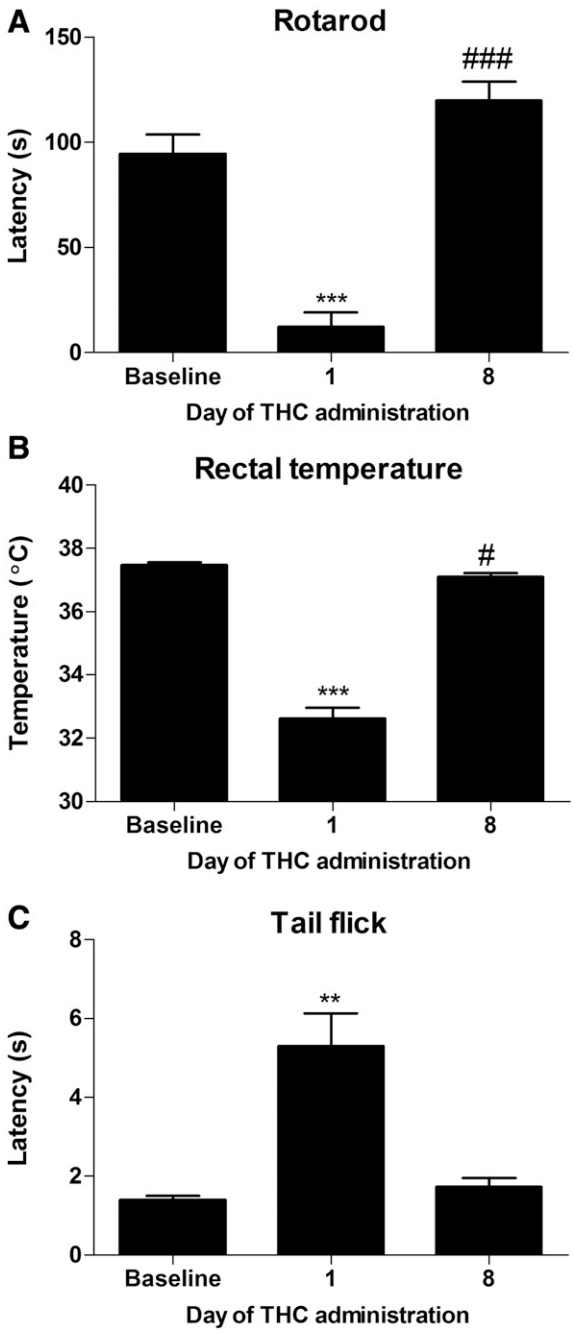

Fig. 7. Mice develop behavioral tolerance to Δ^9-THC administration. Δ^9-THC (50 mg/kg i.p.) produces motor impairment (A), hypothermia (B), and antinociception (C) on day 1 of repeated dosing relative to baseline and day 8 of Δ^9-THC administration (A–C), indicating that mice had become tolerant to the pharmacologic effects of Δ^9-THC. Data are expressed as mean ± S.E.M. (n = 12 C57BL/6J male mice). $^{**}P < 0.01$; $^{***}P < 0.0001$ vs. baseline or day 8; $^{\#}P < 0.05$; $^{\#\#\#}P < 0.0001$ vs. baseline, paired-samples t test.

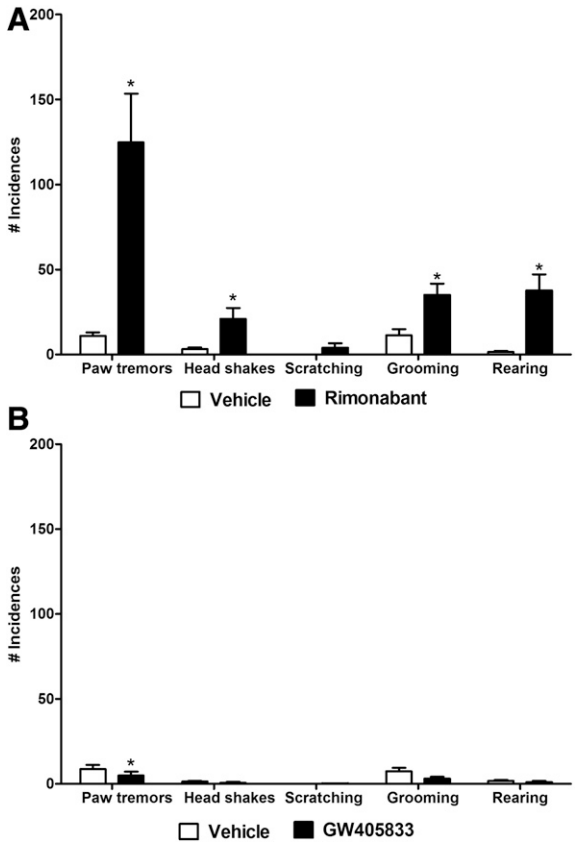

Fig. 8. Rimonabant challenge elicits cannabinoid CB_1-dependent withdrawal behaviors, whereas GW405833 does not. Rimonabant (10 mg/kg i.p.) challenge increases the number of paw tremors, headshakes, grooming, and rearing behaviors in mice chronically treated with Δ^9-THC (see tolerance development for these mice in Fig. 7). (A) GW405833 (10 mg/kg i.p.) decreases the levels of paw tremors in mice chronically treated with Δ^9-THC. (B) Data are expressed as mean ± S.E.M. (n = 6 C57BL/6J male mice per group). $^{*}P < 0.05$ vs. vehicle, paired-samples t test.

GW405833 was absent in CB_1 KO mice and blocked in WT mice by the CB_1 antagonist rimonabant. In neuropathic WT mice, the CB_2 antagonist SR144528 (10 mg/kg i.p.) produced only a modest attenuation of the antiallodynic efficacy of GW405833 (30 mg/kg i.p.); antiallodynic efficacy was suppressed to a level comparable to that of a fully efficacious lower dose (10 mg/kg i.p.). Moreover, the antiallodynic efficacy of GW405833 was not blocked at all by SR144528 in the CFA model. The antinociceptive effects of GW405833 are widely believed to be CB_2 receptor-mediated because of the high selectivity of GW405833 to CB_2 receptor over CB_1 receptor described in vitro (Valenzano et al., 2005), reports of blockade of GW405833 effects by a CB_2 antagonist (Clayton et al., 2002; Beltramo et al., 2006), and an absence of GW405833 antinociceptive efficacy in CB_2KO mice (Valenzano et al., 2005); however, our results suggest that GW405833 does not behave as a CB_2 agonist in mice after systemic administration.

Strikingly, the antiallodynic effects of GW405833 observed in the current study were CB_1 receptor-mediated. These observations are consistent with a previous report suggesting that the antinociceptive effects of GW405833 on lactic acid-induced nociceptive stretch responses were partially blocked by the CB_1 antagonist rimonabant but not by the CB_2 antagonist SR144528 (Kwilasz and Negus, 2013). In the few studies suggesting that the antinociceptive effects of GW405833 are CB_2-mediated (Clayton et al., 2002; Valenzano et al., 2005; Beltramo et al., 2006), neither CB_1 antagonists nor CB_1KOs were used to investigate the possible contribution of CB_1 receptors to the in vivo antinociceptive profile of GW405833. Only one prior study included CB_2KO mice (Valenzano et al., 2005). To our knowledge, our study is the first to include CB_1KO mice to study possible involvement of CB_1 receptors in

the antiallodynic effects of GW405833. GW405833 has been reported to behave as a partial agonist of the orphan G protein–coupled receptor 55 (GPR55) in evaluating L-α-lysophosphatidylinostiol–induced mitogen-activated protein kinase activation in vitro (Anavi-Goffer et al., 2012). It is unclear, however, how GPR55 agonism would produce antinociception. The involvement of GPR55 in pain is controversial (Staton et al., 2008; Carey et al., 2017) and difficult to address owing to the lack of sufficiently selective agonists and antagonists for this receptor.

In the two studies in which the CB_2 antagonist SR144528 was used to block the antinociceptive effect of GW405833 (Clayton et al., 2002; Beltramo et al., 2006), different pain models (i.e., carrageenan and formalin inflammatory pain models), different methods (i.e., weight bearing, paw edema, paw licking, and flinching), and different species (i.e., rats were used by Clayton and colleagues) were used compared with our study; these differences may have contributed to the different pattern of results obtained. One possibly noteworthy difference in methods is that GW405833 was administered before the noxious insult in both prior studies, whereas in our study, GW405833 was administered after the establishment of both neuropathic pain and inflammatory pain. Thus, it is possible that GW405833 blocks pain through a CB_2-mediated mechanism during the development of pain but through a CB_1-mediated mechanism during the maintenance of pathologic pain. In the study by Valenzano et al. (2005), the antiallodynic effect of GW405833 (30 mg/kg i.p.) in the CFA model in CB_2KO mice is reported to not differ from vehicle; however, this latter study did not evaluate whether the efficacy of GW405833 differed statistically in WT and CB_2KO mice. Inadequate statistical power could account for failure to observe differences in responding between CB_2KO mice receiving vehicle and GW405833 at the single time point evaluated previously (Valenzano et al., 2005). By contrast, in our study, GW405833 exhibited similar antiallodynic effects in CB_2KO and WT mice at doses of 10 mg/kg i.p. and 30 mg/kg i.p. Both our study and that of Valenzano et al. (2005) used CB_2KO mice on the C57BL/6 background and the same concentration of CFA in the paw (20 μl, 50% CFA diluted in 0.9% saline). The effect of GW405833 (30 mg/kg i.p.) was studied 24 hours after CFA injection by Valenzano et al., whereas in our study, GW405833 was tested $\geq$48 hours after CFA injection. If GW405833 engages different antinociceptive mechanisms during different stages of the maintenance of inflammatory pain, then inclusion of different testing time points between studies could potentially contribute to the observed discrepancies.

Although GW405833 binds with higher affinity to the orthosteric site on CB_2 receptors relative to CB_1 receptors in vitro, the degree of selectivity for CB_2 over CB_1 is quite variable among studies, ranging from 37-fold up to ~1200-fold selective to human CB_2 receptors over human CB_1 receptors (Gallant et al., 1996; Valenzano et al., 2005; Yao et al., 2008). Although it is possible that species differences exist between rat and mouse CB_2 receptors, they are much more highly conserved compared with human CB_2 receptors (Liu et al., 2009). Binding of GW405833 to native mouse CB_2 receptors, to our knowledge, has never been determined. Considering that GW405833 penetrates into the CNS at high levels (Valenzano et al., 2005; Evens et al., 2011), cannabimimetic CB_1-like effects could be expected in the tetrad tests if GW405833 binds directly to the orthosteric binding site of CB_1 receptors; however, the highest effective dose of GW405833 (30 mg/kg i.p.) identified in the present study was inactive in the tetrad tests. Specifically, GW405833 (30 mg/kg i.p.) did not produce catalepsy, motor ataxia, hypothermia, or acute antinociception in the tail-flick test in mice. These observations are in agreement with prior studies (Valenzano et al., 2005; Whiteside et al., 2005) suggesting that GW405833 did not produce cannabimimetic effects at doses lower than 100 mg/kg i.p. A recent study has shown that GW405833 can act as a noncompetitive CB_1 antagonist in vitro, because it noncompetitively antagonized CP55,940-induced adenylyl cyclase inhibition, extracellular signal-regulated kinase 1/2 phosphorylation, phosphatidylinositol 2 signaling, and CB_1 internalization in vitro (Dhopeshwarkar et al., 2017). In addition, GW405833 induced a complex, time-dependent activation of arrestin through CB_1 (Dhopeshwarkar et al., 2017).Therefore, to assess whether GW405833 behaves as an orthosteric CB_1 antagonist in vivo, we evaluated whether challenge with GW405833 would induce CB_1-dependent cannabinoid withdrawal in mice treated chronically with Δ^9-THC (50 mg/kg, i.p. $\times$9 days). In contrast to challenge with the classic CB_1 antagonist/inverse agonist rimonabant (10 mg/kg, i.p.), challenge with GW405833 (10 mg/kg, i.p.) did not induce classic withdrawal responses in THC-tolerant mice. The lack of precipitated withdrawal by GW405833 observed in our withdrawal assay indicates that GW405833 does not behave as a CNS-penetrant competitive CB_1 antagonist in vivo. Thus, caution must be exerted before attributing the mechanism of action underlying in vivo effects of novel ligands to mechanisms identified in vitro.

In summary, the antiallodynic effect of GW405833 in the established neuropathic and inflammatory pain models examined here is CB_1-mediated and not CB_2-mediated. The antiallodynic effects of GW405833 were absent in CB_1KO mice and blocked by a CB_1 antagonist but were fully preserved in CB_2KO mice and largely unaffected by a CB_2 antagonist. Although GW405833 is brain penetrant (Valenzano et al., 2005) and reduced neuropathic and inflammatory pain through a CB_1-mediated mechanism in our study, it did not induce cannabimimetic CB_1-mediated side effects at the highest therapeutic dose evaluated (30 mg/kg i.p.). Moreover, GW405833 (10 mg/kg i.p.) did not function as a competitive CB_1 antagonist in our attempts to precipitate withdrawal with this agent in Δ^9-THC tolerant mice. Together, our results indicate that GW405833 reversed established neuropathic and inflammatory pain through a CB_1-mediated mechanism without producing characteristic cannabimimetic effects associated with direct orthosteric binding to the CB_1 receptor. GW405833 could possibly act as a CB_1 allosteric modulator or interact with the endocannabinoid system. More research is needed to elucidate the mechanism of antinociceptive actions of GW405833.

Authorship Contributions

Participated in research design: Hohmann.

Conducted experiments: Li, Carey.

Performed data analysis: Li, Carey.

Wrote or contributed to the writing of the manuscript: Li, Carey, Mackie, Hohmann.

References

Anavi-Goffer S, Baillie G, Irving AJ, Gertsch J, Greig IR, Pertwee RG, and Ross RA (2012) Modulation of L-α-lysophosphatidylinositol/GPR55 mitogen-activated protein kinase (MAPK) signaling by cannabinoids. *J Biol Chem* **287**:91–104.

Atwood BK and Mackie K (2010) CB2: a cannabinoid receptor with an identity crisis. *Br J Pharmacol* **160**:467–479.

Beltramo M, Bernardini N, Bertorelli R, Campanella M, Nicolussi E, Fredduzzi S, and Reggiani A (2006) CB2 receptor-mediated antihyperalgesia: possible direct involvement of neural mechanisms. *Eur J Neurosci* **23**:1530–1538.

Bouchard J, Truong J, Bouchard K, Dunkelberger D, Desrayaud S, Moussaoui S, Tabrizi SJ, Stella N, and Muchowski PJ (2012) Cannabinoid receptor 2 signaling in peripheral immune cells modulates disease onset and severity in mouse models of Huntington's disease. *J Neurosci* **32**:18259–18268.

Brownjohn PW and Ashton JC (2012) Spinal cannabinoid CB2 receptors as a target for neuropathic pain: an investigation using chronic constriction injury. *Neuroscience* **203**:180–193.

Carey LM, Gutierrez T, Deng L, Lee W-H, Mackie K, and Hohmann AG (2017) Inflammatory and neuropathic nociception is preserved in GPR55 knockout mice. *Sci Rep* **7**:944.

Clayton N, Marshall FH, Bountra C, and O'Shaughnessy CT (2002) CB1 and CB2 cannabinoid receptors are implicated in inflammatory pain. *Pain* **96**:253–260.

Dhopeshwarkar A, Murataeva N, Makriyannis A, Straiker A, and Mackie K (2017) Two Janus cannabinoids that are both CB2 agonists and CB1 antagonists. *J Pharmacol Exp Ther* **360**:300–311.

Evens N, Vandeputte C, Muccioli GG, Lambert DM, Baekelandt V, Verbruggen AM, Debyser Z, Van Laere K, and Bormans GM (2011) Synthesis, in vitro and in vivo evaluation of fluorine-18 labelled FE-GW405833 as a PET tracer for type 2 cannabinoid receptor imaging. *Bioorg Med Chem* **19**:4499–4505.

Galiègue S, Mary S, Marchand J, Dussossoy D, Carrière D, Carayon P, Bouaboula M, Shire D, Le Fur G, and Casellas P (1995) Expression of central and peripheral cannabinoid receptors in human immune tissues and leukocyte subpopulations. *Eur J Biochem* **232**:54–61.

Gallant M, Dufresne C, Gareau Y, Guay D, Leblanc Y, Prasit P, Rochette C, Sawyer N, Slipetz DM, Tremblay N, et al. (1996) New class of potent ligands for the human peripheral cannabinoid receptor. *Bioorg Med Chem Lett* **6**:2263–2268.

Guindon J and Hohmann AG (2008) Cannabinoid CB2 receptors: a therapeutic target for the treatment of inflammatory and neuropathic pain. *Br J Pharmacol* **153**: 319–334.

Guindon J and Hohmann AG (2009) The endocannabinoid system and pain. *CNS Neurol Disord Drug Targets* **8**:403–421.

Herkenham M, Lynn AB, Johnson MR, Melvin LS, de Costa BR, and Rice KC (1991) Characterization and localization of cannabinoid receptors in rat brain: a quantitative in vitro autoradiographic study. *J Neurosci* **11**:563–583.

Hu B, Doods H, Treede RD, and Ceci A (2009) Depression-like behaviour in rats with mononeuropathy is reduced by the CB2-selective agonist GW405833. *Pain* **143**: 206–212 International Association for the Study of Pain.

Ibrahim MM, Porreca F, Lai J, Albrecht PJ, Rice FL, Khodorova A, Davar G, Makriyannis A, Vanderah TW, Mata HP, et al. (2005) CB2 cannabinoid receptor activation produces antinociception by stimulating peripheral release of endogenous opioids. *Proc Natl Acad Sci USA* **102**:3093–3098.

Iversen L and Chapman V (2002) Cannabinoids: a real prospect for pain relief? *Curr Opin Pharmacol* **2**:50–55.

Kwilasz A, and Negus S (2013) Effects of the cannabinoid 2 receptor-selective agonist GW405833 in assays of acute pain-stimulated and paindepressed behavior in rats. *FASEB J* **27**:886.9.

LaBuda CJ, Koblish M, and Little PJ (2005) Cannabinoid CB2 receptor agonist activity in the hindpaw incision model of postoperative pain. *Eur J Pharmacol* **527**: 172–174.

Leichsenring A, Andriske M, Bäcker I, Stichel CC, and Lübbert H (2009) Analgesic and antiinflammatory effects of cannabinoid receptor agonists in a rat model of neuropathic pain. *Naunyn Schmiedebergs Arch Pharmacol* **379**:627–636.

Liu Q-R, Pan C-H, Hishimoto A, Li C-Y, Xi Z-X, Llorente-Berzal A, Viveros M-P, Ishiguro H, Arinami T, Onaivi ES, et al. (2009) Species differences in cannabinoid receptor 2 (CNR2 gene): identification of novel human and rodent CB2 isoforms, differential tissue expression, and regulation by cannabinoid receptor ligands. *Genes Brain Behav* **8**:519–530.

Mancini I, Brusa R, Quadrato G, Foglia C, Scandroglio P, Silverman LS, Tulshian D, Reggiani A, and Beltramo M (2009) Constitutive activity of cannabinoid-2 (CB2) receptors plays an essential role in the protean agonism of (+)AM1241 and L768242. *Br J Pharmacol* **158**:382–391.

Matsuda LA, Lolait SJ, Brownstein MJ, Young AC, and Bonner TI (1990) Structure of a cannabinoid receptor and functional expression of the cloned cDNA. *Nature* **346**:561–564.

Munro S, Thomas KL, and Abu-Shaar M (1993) Molecular characterization of a peripheral receptor for cannabinoids. *Nature* **365**:61–65.

Pertwee RG (1972) The ring test: a quantitative method for assessing the 'cataleptic' effect of cannabis in mice. *Br J Pharmacol* **46**:753–763.

Rahn EJ, Zvonok AM, Makriyannis A, and Hohmann AG (2010) Antinociceptive effects of racemic AM1241 and its chirally synthesized enantiomers: lack of dependence upon opioid receptor activation. *AAPS J* **12**:147–157.

Staton PC, Hatcher JP, Walker DJ, Morrison AD, Shapland EM, Hughes JP, Chong E, Mander PK, Green PJ, Billinton A, et al. (2008) The putative cannabinoid receptor GPR55 plays a role in mechanical hyperalgesia associated with inflammatory and neuropathic pain. *Pain* **139**:225–236.

Valenzano KJ, Tafesse L, Lee G, Harrison JE, Boulet JM, Gottshall SL, Mark L, Pearson MS, Miller W, Shan S, et al. (2005) Pharmacological and pharmacokinetic characterization of the cannabinoid receptor 2 agonist, GW405833, utilizing rodent models of acute and chronic pain, anxiety, ataxia and catalepsy. *Neuropharmacology* **48**:658–672.

Viscomi MT, Oddi S, Latini L, Pasquariello N, Florenzano F, Bernardi G, Molinari M, and Maccarrone M (2009) Selective CB2 receptor agonism protects central neurons from remote axotomy-induced apoptosis through the PI3K/Akt pathway. *J Neurosci* **29**:4564–4570.

Whiteside GT, Gottshall SL, Boulet JM, Chaffer SM, Harrison JE, Pearson MS, Turchin PI, Mark L, Garrison AE, and Valenzano KJ (2005) A role for cannabinoid receptors, but not endogenous opioids, in the antinociceptive activity of the CB2-selective agonist, GW405833. *Eur J Pharmacol* **528**:65–72.

Yao BB, Mukherjee S, Fan Y, Garrison TR, Daza AV, Grayson GK, Hooker BA, Dart MJ, Sullivan JP, and Meyer MD (2006) In vitro pharmacological characterization of AM1241: a protean agonist at the cannabinoid CB2 receptor? *Br J Pharmacol* **149**:145–154.

Yao BB, Hsieh GC, Frost JM, Fan Y, Garrison TR, Daza AV, Grayson GK, Zhu CZ, Pai M, Chandran P, et al. (2008) In vitro and in vivo characterization of A-796260: a selective cannabinoid CB2 receptor agonist exhibiting analgesic activity in rodent pain models. *Br J Pharmacol* **153**:390–401.

Zhang J, Hoffert C, Vu HK, Groblewski T, Ahmad S, and O'Donnell D (2003) Induction of CB2 receptor expression in the rat spinal cord of neuropathic but not inflammatory chronic pain models. *Eur J Neurosci* **17**:2750–2754.

Zimmermann M (1983) Ethical guidelines for investigations of experimental pain in conscious animals. *Pain* **16**:109–110.

Address correspondence to: Andrea G. Hohmann, Department of Psychological and Brain Sciences, Indiana University, 1101 E 10th Street, Bloomington, IN 47405-7007. E-mail: hohmanna@indiana.edu